CHAPTER II

EXPERIMENTAL DETAILS

II.1 Instruments

Leitz WETZLAR 543594 heating-stage microscope with 8x1.25x10, 8x1.25x32 magnifications, polarizer and analyser

Reichert heating-stage microscope with 10x10 magnification, polarizer and analyser

Power supply : SHANDON VOKAM 2541, Type M303 No. L12581

Voltmeter THAI RADIO 170TR

Rotary Regavolt Transformers, Series 70, Type 71C and 72C

Pentax Camera and Pentax adapter

Kodak Tri-X Pan Films, 36 mm, ASA400 (DIN27)

II.2 Chemicals

II.2.1 Nematic liquid crystals

EPPHX : p-(p-Ethoxyphenylazo) phenyl hexanoate (Eastman-Kodak catalogue number 10537)

PPAB : 4,4-Bis(pentyloxy) azoxybenzene (Eastman-Kodak catalogue number 10715)

PCBA : N-(p-(pentyloxycarbonyloxy) benzylidene) p-anisidine (Eastman-Kodak catalogue number 11479)

EPAPV : p-(p-Ethoxyphenylazo)phenyl valerate (Eastman-Kodak catalogue number 10901)

EPPHP : p-(p-Ethoxyphenylazo)phenyl heptanoate (Eastman-Kodak catalogue number 10573)

II.2.2 Smectic liquid crystals

PCBAV : 4-((p-Pentyloxycarbonyloxybenzylidene)amino) valerophenone (Eastman-Kodak catalogue number 11441)

EEBAC : Ethyl-p-((p-ethoxybenzylidene)amino)cinnamate (Eastman-Kodak catalogue number 922808)

EMBAC : Ethyl-p((p-methoxybenzylidene)amino)cinnamate (Eastman-Kodak catalogue number 10306)

Stannic chloride ($SnCl_4.5H_2O$), antimony pentachloride and ethyl acetate

II.3 Preparation of Electro-Optical Cells with Transparent Electrodes and Free-Lead Electrodes

II.3.1 Cells with transparent electrodes

Microscope glass slides (2.5x7.6 cm^2) were dipped in the cleaning solution for 6-10 hours and washed with water. These glass slides were then placed on a hot plate and were heated up to and maintained at a temperature above 300 ^{o}C. A solution of stannic acetate was prepared from 49.8g of $SnCl_4.5H_2O$, 33.3 ml of ethyl acetate, 1 ml of $SbCl_5$ and 7.6 ml of H_2O. This solution, immediately after preparation, was applied by spraying onto only one side of the heated glass slides to obtain uniform thin conductive films. Fine

sprays, each lasting about 1-5 seconds, were made at intervals of at least 15 seconds in order to maintain the temperature above 300°C . When thin films of stannic oxide were of suitable thickness, their electrical resistance should be about 100-150 ohms.

The edges of these conductive coated slides were ground with emery paper to prevent electric discharge through edges. Each slide was then cut into two equal pieces and these were used as transparent electrodes. Each sample cell was made up of a pair of conductive slides coated with a conductive layer on the inner sides. A small drop of liquid crystal was sandwiched between the slides and was held quite firmly between these electrodes. Two pieces of aluminium foil were used for electrical contact between the cell and the external circuit. The electrodes were separated by Mylar films of 80 μm thickness. This cell was attached onto an ordinary glass slide with the aid of Duco cement.

II.3.2 Cells with free-lead electrodes

Two aluminium strips of 20 μm thickness were attached to a glass slide with separation of about 0.3 mm. The thickness of the electrodes was varied either by replacing the aluminium strips with two bare copper wires or by doubling the thickness of the aluminium strips. A drop of nematic or smectic liquid crystal was placed between the electrodes and covered with a piece of cover slip.

II.4 Electrical Circuit

A.C. voltages were supplied by a transformer. Voltages at frequencies other than 50 Hz were obtained from

electronic oscillator. The electric field used ranged from zero to about 2.5×10^4 volts/cm in the transparent-electrodes configuration and to about 10^3 volts/cm in the free-lead-electrodes configuration. D.C. voltages were obtained from a standard voltage supply.

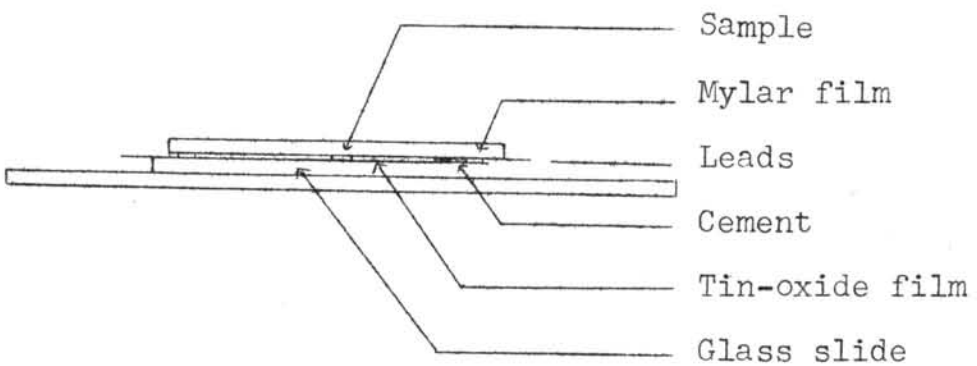

Fig.1a Side view of a schematic diagram of an electro-optical cell with transparent electrodes

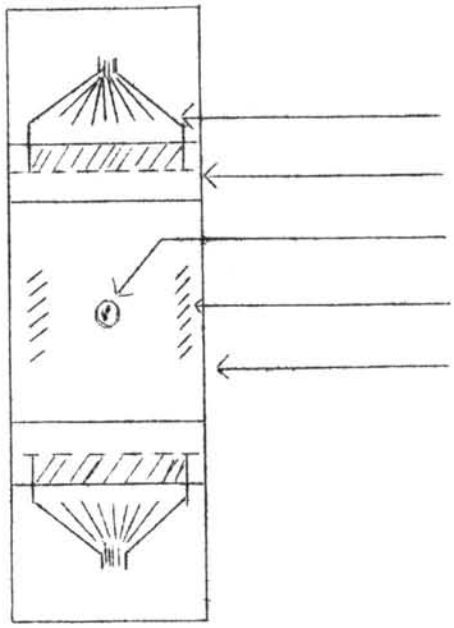

Fig.1b Top view of a schematic diagram of an electro-optical cell with transparent electrodes

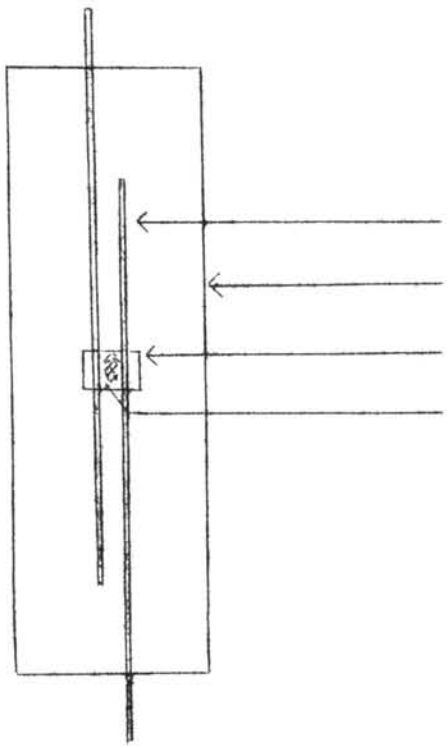

Fig.2 Schematic diagram of an electro-optical cell with free-lead electrodes

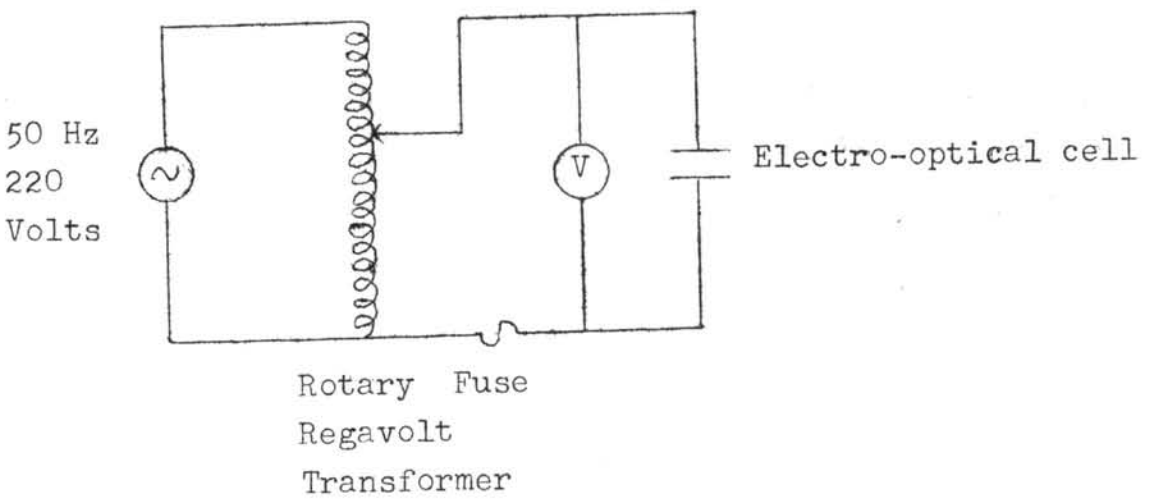

Fig.3a a.c. circuit

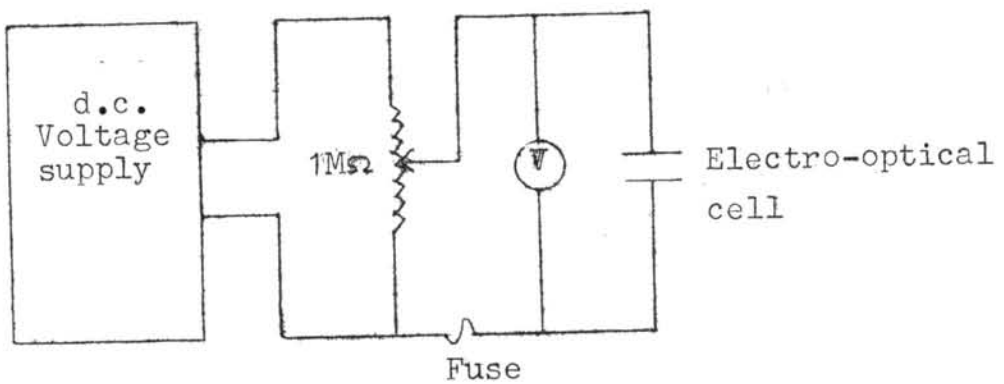

Fig.3b d.c. circuit

II.5 Experimental Methods

The electrohydrodynamics of five nematic and three smectic liquid crystals under the influence of an electric field was investigated in detail at various field strengths in the range of zero and 10^4 volts/cm. D.C. and 50 Hz a.c. electric field were applied in studying the motions of liquid crystals placed in the electro-optical cell with both types of electrodes. The visible patterns obtained in the presence of an electric field were observed through a **Leitz** heating-stage microscope with 100 x and 320 x magnifications and also through a Reichert heating-stage microscope with 100 x magnification. Photographs of the visible patterns were taken by using a Pentax camera. Very sensitive photographic films with ASA number of 400 (DIN27) were used to reduce exposure times to 1/4, 1/8, and 1/15 seconds.

II.6 Experimental Results

II.6.1 Transition temperatures

Transition temperatures of liquid crystals were calibrated against those of standard compounds and are listed in Tables 1 and Table 2

Table 1 Transition temperatures of nematic liquid crystals

Liquid crystal	T(K-N) $^{\circ}$ C	T(N-I) $^{\circ}$ C
EPPHX	71.1±0.2	123.4±0.2
EPPHP	60.0±0.2	112.6±0.2
EPAPV	75.9±0.2	122.0±0.2
PPAB	76.5±0.2	116.6±0.2
PCBA	58.1±0.2	76.9±0.2

Table 2 Transition temperatures of smectic liquid crystals

Liquid crystal	T(K-S) ^{o} C	T(S-N) ^{o} C	T(S-I) ^{o}C	T(N-I) ^{o}C
PCBAV	75.5±0.2	-	110.3±0.2	-
EEBAC	73.5±0.2	147.3±0.2	-	149.2±0.2
EMBAC	102.5±0.2	113.5±0.2	-	134.4±0.2

K for solid, N nematic, S smectic and I isotropic

II.6.2 The threshold fields for formation of domains

The threshold values for both a.c. and d.c. fields for onset of the Williams domains in nematic liquid crystals between transparent electrodes are listed in Table 3

Table 3 Threshold fields for the formation of domains

Liquid crystal	a.c.Threshold field(volts/cm)	d.c.Threshold field(volts/cm)	Temperature(^{o}C)
EPPHX	1.6×10^{3}	$\sim$ 0	91.4±0.5
EPPHP	2.4×10^{3}	5.0×10^{3}	71.8±0.5
EPAPV	8.5×10^{2}	1.0×10^{3}	90.0±0.5
PPAB	1.4×10^{3}	1.5×10^{3}	91.9±0.5
PCBA	8.5×10^{2}	1.7×10^{3}	90.0±0.5

It should be noted as illustrated by the results in Table 3, threshold fields obtained in a.c. electric fields were not necessarily the same as those obtained in d.c. field

II.6.3 Motions of nematic liquid crystals placed between transparent electrodes

As the a.c. field across the transparent electrodes was increased slowly, some fine dark grains first appeared and started to move up and down along the field direction. At the threshold field strength these grains moved in an ordered manner and formed a nearly regular pattern of alternately dark and bright stripes which have already been investigated by Williams[1] and are now widely known as domains of anomalous alignment or Williams domains. The domains could be observed clearly when the polarizations of the polarizer and the analyser were the same and completely disappeared when the two polarizations were crossed. It appeared that the domain size depended only on the thickness of the samples. The liquid crystal layer was divided into alternate regions of dark and much smaller bright stripes. Also, by carefully focusing the microscope on different parts of the domain pattern, it was found that there were in fact two sets of bright domain lines.

The flexibility of the domains was so high that they could be easily distorted by an a.c. field and they frequently formed junctions with adjacent domains. When the field was increased to a value higher than that required for domain formation, the motions became more disordered with some parts of the domains moving up, some moving down. As the field was raised further, a large number of regular polygons occurred, similar to the well

---

[1] R.Williams, "Domains in Liquid Crystals.", J.Chem. Phys.,39 (1963), 384

known Bénard cells[2]. These polygons moved slightly and they all contained dark spots at the center of the cells. More careful observation indicated that these spots were the points at which the material was moving upwards. The cells were bounded by dark boundaries where the material moved downwards.

Generally, the motions in an a.c. field and a d.c. field were quite similar. The distinct characteristics of each nematic liquid crystal used in the experiments are described below.

a) Characteristic behaviours of EPPHX and EPAPV

It was observed that some parts of the domains were hidden behind the nematic texture which occurred in these nematic liquid crystals. The hidden parts of the domains could be investigated by rotating either the polarizer or the analyser. The domain size depended only on the thickness of the samples.

The mobility of the domains in an a.c. field was approximately the same as that in a d.c. field. In both fields, when the temperature was raised the mobility of the domain increased slightly. The characteristic motions of EPPHX are illustrated in Fig.4 at a.c. field of 9.6×10^2 volts/cm, temperature 81.3 ^{o}C, and sample thickness of 80 μm. More disordered motions are shown in Fig.5 at a.c. field of 1.9×10^3 volts/cm, temperature 81.8 ^{o}C and

---

[2] H.Bénard, "Les Tourbillions Cellulaires dans une nappe Liquide Transportant de la Chaleur par Convection en Régime Permanent", Ann.Chim.Phys., 23 (1901), 62

sample thickness of 80 μm. Fig.6 shows the polygonal pattern at d.c. field 1.2×10^4 volts/cm, temperature 129.1 ^{o}C, sample thickness 200 μm.

In EPPHX, the a.c. threshold for domain formation was much higher than that required for d.c. field since the d.c. threshold field was nearly zero. However, in EPAPV the d.c. threshold field was roughly the same as the a.c. threshold. The motions of EPAPV are shown in Fig.7 at a.c. field of 1.6×10^3 volts/cm, temperature 97.2 ^{o}C in Fig.8 at a.c. field of 2.5×10^3 volts/cm, temperature 97.5 ^{o}C, and in Fig.9 and in Fig.10 at a.c. field of 3.8×10^3 volts/cm, temperatures 81.2 ^{o}C and 97.5 ^{o}C, all with sample thickness of 80 μm.

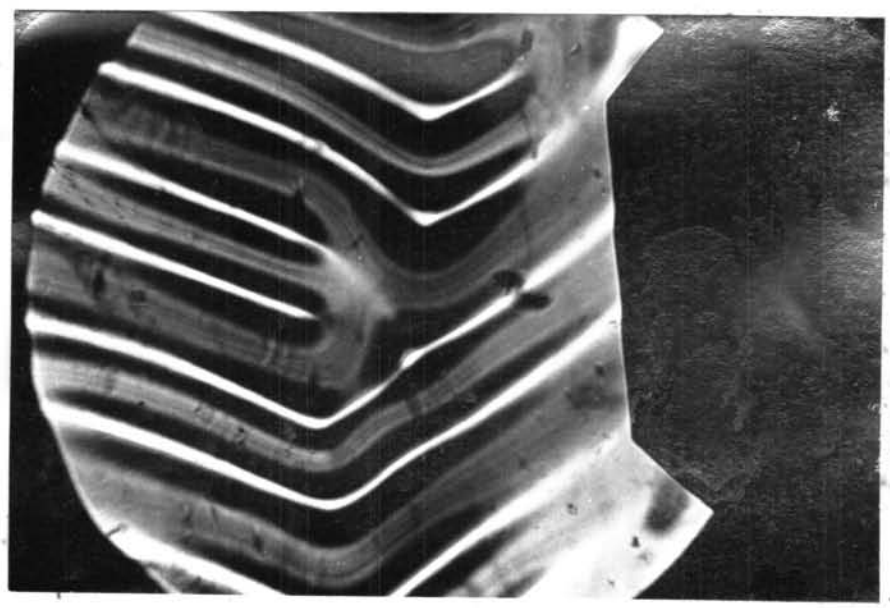

Fig.4 A 80 μm-thick layer of EPPHX placed between transparent electrodes in an a.c. electric field of 9.6×10^2 volts/cm at 81.3 ^{o}C.

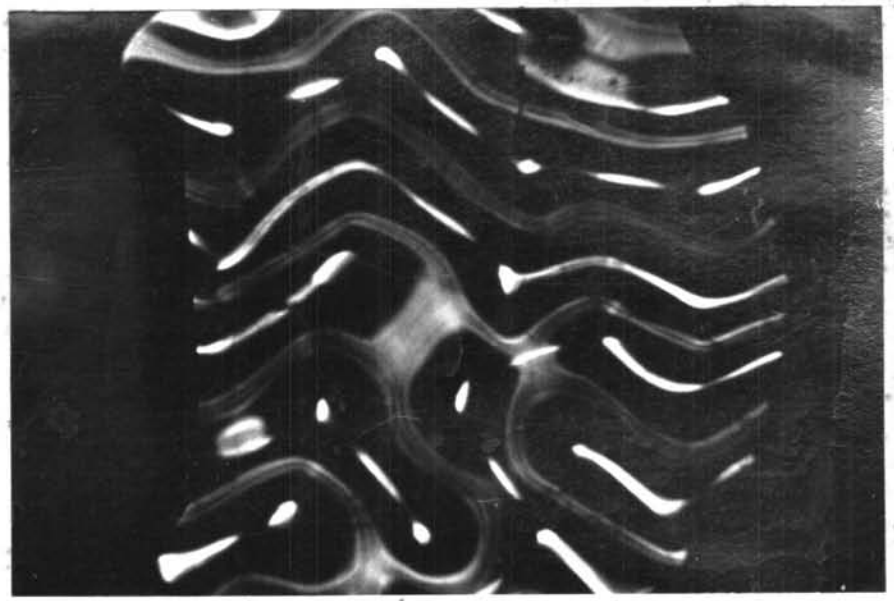

Fig.5 A 80 μm-thick layer of EPPHX placed between transparent electrodes in an a.c. electric field of 1.9×10^3 volts/cm at 81.8 ^{o}C.

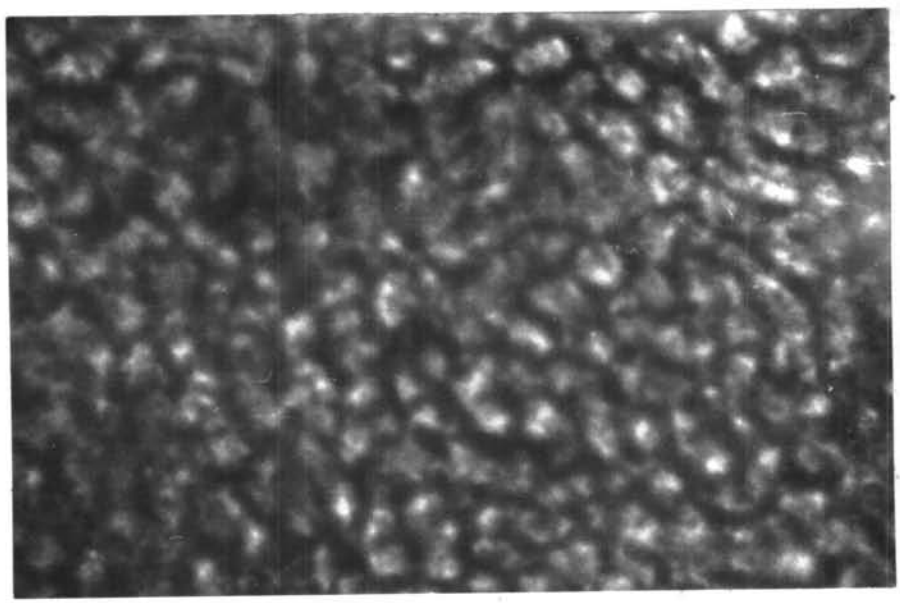

Fig.6 A 200 μm-thick layer of EPPHX placed between transparent electrodes in a d.c. electric field of 1.2×10^4 volts/cm at 129.1 ^{o}C.

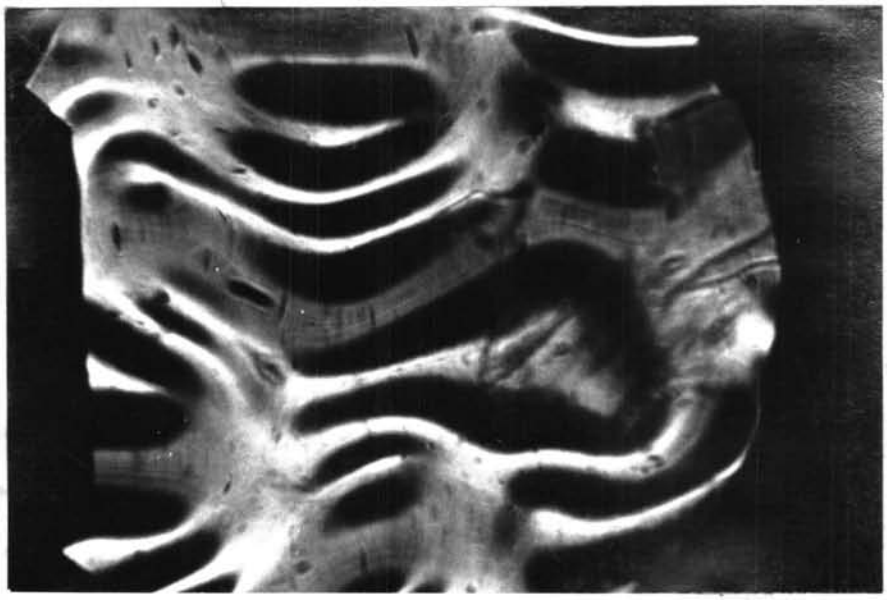

Fig.7 A 80 μm-thick layer of EPAPV placed between transparent electrodes in an a.c. electric field of 1.6×10^3 volts/cm at 97.2 ^{o}C.

Fig.8 A 80 μm-thick layer of EPAPV placed between transparent electrodes in an a.c. electric field of 2.5×10^3 volts/cm at 97.5 ^{o}C.

Fig.9 A 80 μm-thick layer of EPAPV placed between transparent electrodes in an a.c. electric field of 3.8×10^3 volts/cm at 81.2 °C.

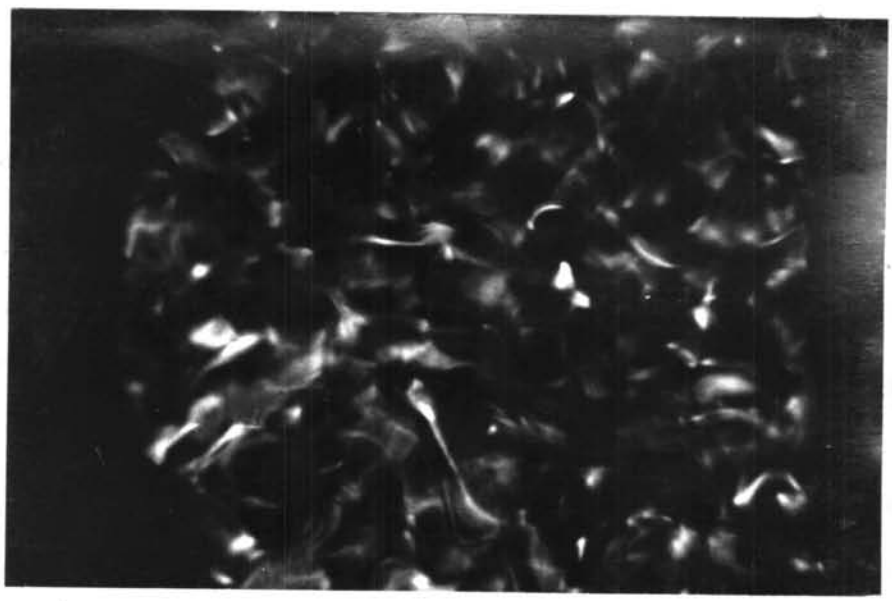

Fig.10 A 80 μm-thick layer of EPAPV placed between transparent electrodes in an a.c. electric field of 3.8×10^3 volts/cm at 97.5 °C.

b) Characteristic behaviours of PPAB

The arrangement of the domains was rather disordered, even when the field was just above the threshold as shown in Fig.11 at a.c. field of 9.4×10^2 volts/cm, temperature 92.7 °C with a sample thickness 80 μm. The domains appeared fairly bright even in the "dark" region.

The domains could persist for several seconds after the field was switched off. The motions were in several respects the same in both the a.c. and d.c. fields. The motion at higher field is shown in Fig.12 at a.c. field of 3.8×10^3 volts/cm, temperature 92.0 °C, with a sample thickness of 80 μm. At a very high field the motion changed to more ordered regular polygons, as illustrated in Fig.13, for an a.c. field of 1.8×10^3 volts/cm, temperature 122.5 °C with a sample thickness of 100 μm. This behaviour could be particularly clearly observed near the nematic-isotropic transition temperature. The size of the polygonal cells became larger as the temperature approached the nematic-isotropic transition temperature.

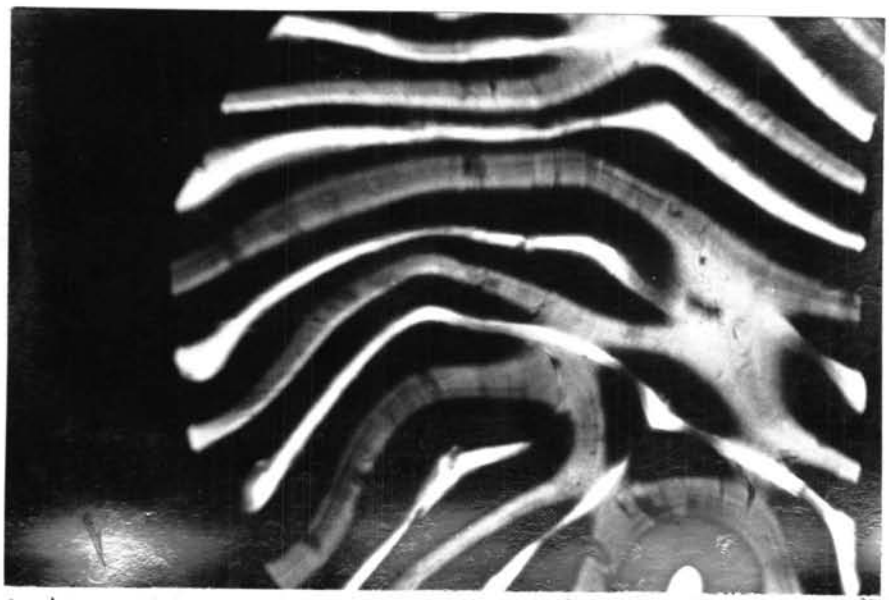

Fig.11 A 80 μm-thick layer of PPAB placed between transparent electrodes in an a.c. electric field of 9.4×10^2 volts/cm at 92.7 °C

Fig.12 A 80 μm-thick layer of PPAB placed between transparent electrodes in an a.c. electric field of 3.8×10^3 volts/cm at 92 °C.

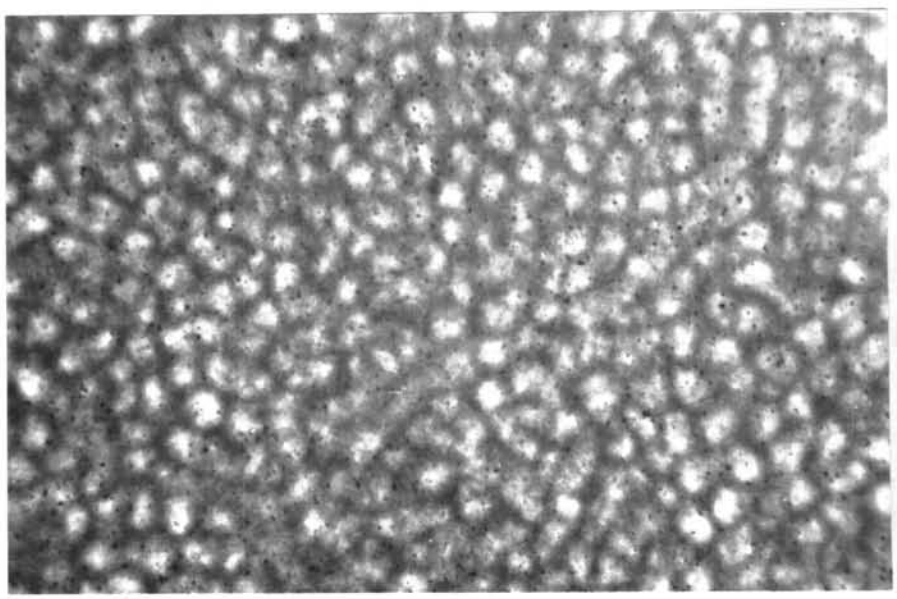

Fig.13 A 100 μm-thick layer of PPAB placed between transparent electrodes in an a.c. electric field of 1.8×10^4 volts/cm at 122.5 °C.

c) Characteristic behaviours of PCBA and EPPHP

The effects of an electric field on these compounds were quite different from those already described in the previous sections. It was found that these liquid crystals showed a higher degree of mobilities in a d.c. field rather than in an a.c. field as illustrated in Fig.14 for EPPHP at d.c. field of 1.0×10^4 volts/cm, temperature 66.6 °C, with a sample thickness 100 μm. The domain pattern was nearly regular and each domain was larger than that observed in other materials, as shown in Fig.15 for EPPHP at a.c. field of 7.5×10^3 volts/cm, temperature 67.1 °C, and sample thickness of 100 μm. The domains were quite stationary at just above the threshold fields, but they changed to more disordered motions at higher fields as illustrated in Fig.16 for EPPHP at a.c. field of 2.0×10^4 volts/cm, temperature 67.1 °C, and in Fig.17 for the same material at d.c. field of 2.5×10^4 volts/cm, temperature 67.1 °C, both with sample thickness of 100 μm.

The decay time and the formation time of the domains were fairly large. After switching off the field it took about 30-60 seconds before the domains completely decayed and it took at least 30 seconds for the domains to appear after switching the field on. The characteristic motions of PCBA are shown in Fig.18 at a.c. field of 2.1×10^3 volts/cm, temperature 69.4 °C, in Fig.19 at a.c. field of 1.0×10^3 volts/cm, temperature 68.1 °C, and the polygonal pattern is shown in Fig.20 at a.c. field of 2.5×10^4 volts/cm, temperature 75.8 °C, all with sample thickness of 100 μm.

Fig.14 A 100 μm-thick layer of EPPHP placed between transparent electrodes in a d.c. electric field of 1.0×10^4 volts/cm at 66.6 °C.

Fig.15 A 100 μm-thick layer of EPPHP placed between transparent electrodes in an a.c. electric field of 7.5×10^3 volts/cm at 67.1 °C.

Fig.16 A 100 μm-thick layer of EPPHP placed between transparent electrodes in an a.c. electric field of 2.0×10^4 volts/cm at 67.1 ^{o}C.

Fig.17 A 100 μm-thick layer of EPPHP placed between transparent electrodes in a d.c. electric field of 2.5×10^4 volts/cm at 67.1 ^{o}C.

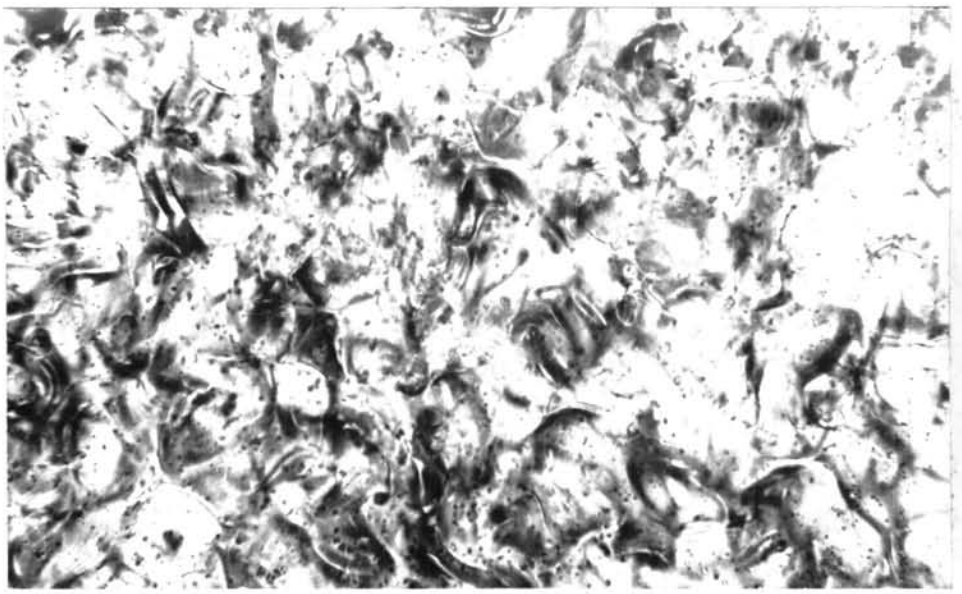

Fig.18 A 100 μm-thick layer of PCBA placed between transparent electrodes in an a.c. electric field of 2.1×10^3 volts/cm at 69.4 ^{o}C.

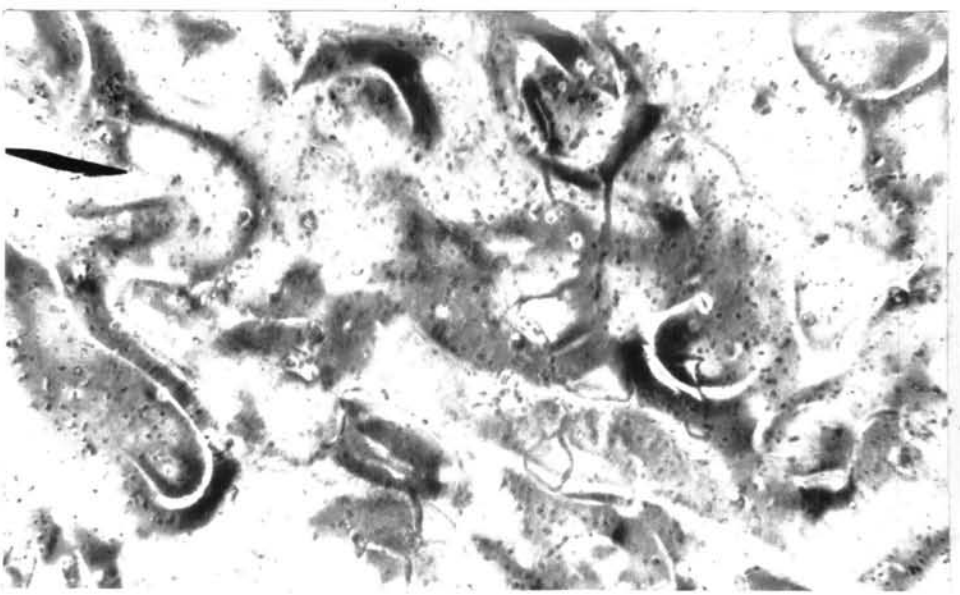

Fig.19 A 100 μm-thick layer of PCBA placed between transparent electrodes in an a.c. electric field of 1.0×10^3 volts/cm at 68.1 ^{o}C.

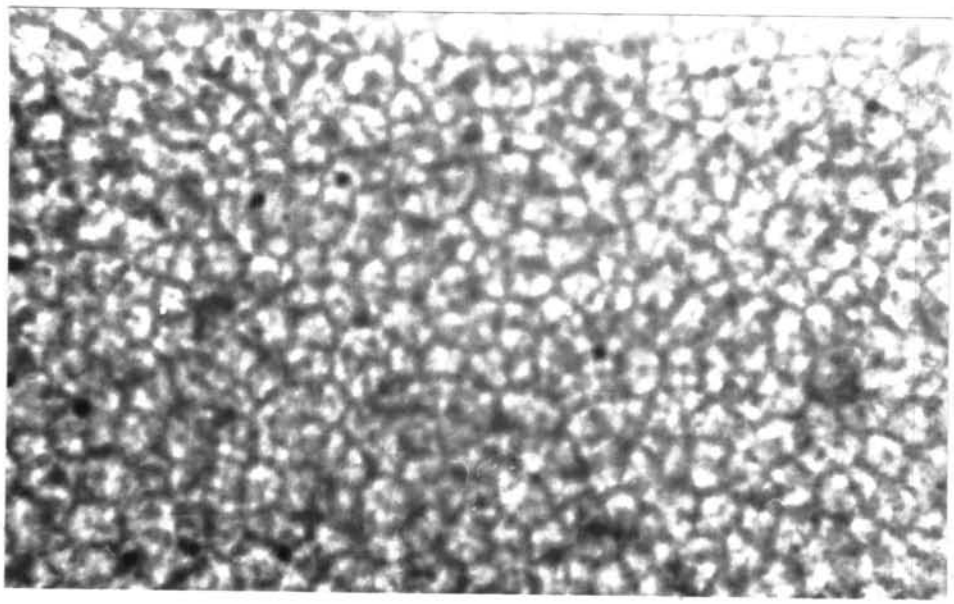

Fig.20 A 100 μm-thick layer of PCBA placed between transparent electrodes in an a.c. electric field of 2.5×10^4 volts/cm at 75.8 °C.

II.6.4 Motions of nematic liquid crystals placed between free-lead electrodes

Voltage was applied across the electrodes of an electro-optic cell which contained a drop of a nematic liquid crystal, and was gradually increased. After a short time fine dark grains appeared in the nematic material, oscillating between the electrodes. As the voltage was increased further to a fairly sharp threshold field, these fine grains produced a very interesting pattern of dark and bright stripes. This anomalous pattern consisted of long cylinders with bright much smaller cylinders inside and it would be also appropriate to call them "domains". There could be two sets of domains if the sample layer was thick enough for their existence. In the fine structure of the domains, it could be observed that the dark grains oscillated very

rapidly in the dark stripes. This kind of motion could also occur in the bright stripes, especially at the apices of the domains.

Initially, just above the threshold field, the domains were stationary, starting off from each electrode and disappearing somewhere in the region between the electrodes. The domains from one electrode moved in the direction opposite to and were aligned alternately to those from the other electrode. A typical illustration is shown in Fig.21 for EPAPV in an a.c. field of 6.4×10^2 volts/cm, temperature 90.6 ^{o}C, with a sample thickness of 150 μm. At higher field strengths, the domains could reach the electrodes before they disappeared. At such field strengths, the motions were more vigorous and the domains were more irregular and more highly flexible, as shown in Fig.22 for EPAPV in an a.c. field of 2.1×10^3 volts/cm, temperature 91.6 ^{o}C, with sample thickness of 150 μm. Frequently, the domains broke into shorter rods which still moved towards the electrodes.

The number of the domains were strongly dependent on the field strength. However, their size appeared to depend only on the thickness of the samples. On the other hand the domains could be observed at any temperature in the nematic phase. It was found that at higher temperatures the domains showed slightly higher mobility.

The domains were partially masked behind the nematic texture because the transmitted light was polarized in a definite manner after passing through the texture. The hidden parts could be viewed by rotating either the polarizer or the analyser. The domains completely disappeared in crossed polarizers, and would reappear if either the polarizer or the analyser was rotated further.

The motions of the nematic liquid crystals in a d.c. field were in some aspects different from those described in the case of an a.c. field. In a d.c. field, it was found that the domains were in general more flexible, more strongly-curved, and frequently moved backwards to the same electrode, as shown in Fig.23 for EPAPV in a d.c. field of 6.4×10^2 volts/cm, temperature 92.0 °C, and sample thickness 150 μm. Some domains could occasionally form junctions with adjacent domains. The motions were also more disordered in a d.c. field, as illustrated in Fig.24 for EPAPV in a d.c. field 1.8×10^3 volts/cm, temperature 92.0 °C with a sample thickness of 150 μm. The d.c. threshold field for the domain formation may be either higher or lower than that for the d.c. field depending on the particular liquid crystals used in the experiments.

Fig.21 A 150 μm-thick layer of EPAPV in an a.c. electric field of 6.4×10^2 volts/cm at 90.6 °C with the free-lead electrodes having separation of 1.18 mm.

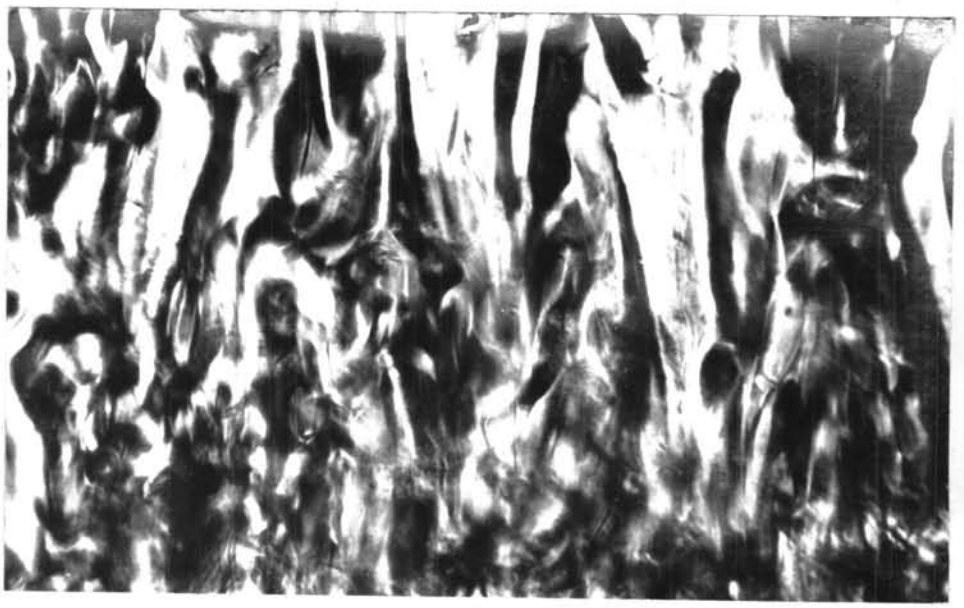

Fig.22 A 150 μm-thick layer of EPAPV in an a.c. electric field of 2.1×10^3 volts/cm at 91.6 °C with the free-lead electrodes having separation of 1.18 mm.

Fig.23 A 150 μm-thick layer of EPAPV in a d.c. electric field of 6.4×10^2 volts/cm at 92.0 °C with the free-lead electrodes having separation of 1.18 mm.

Fig.24 A 150 μm-thick layer of EPAPV in a d.c. electric field of 1.8×10^3 volts/cm at 92.0 °C with the free-lead electrodes having separation of 1.18 mm.

II.6.5 Textures of smectic liquid crystals

When a smectic liquid crystal was heated to the solid-smectic transition temperature and its texture was observed through the polarizing microscope, the melted liquid-crystal layer appeared to be divided into a number of small focal-conic regions separated by sharp boundaries. A particular modification of the basic focal-conic textures, the fan-shaped texture, that was generally obtained under this condition, consisted of long axially-symmetric regions, each with an optically active apex. These regions could differ very widely in size. In crossed polaroids, each region was uniformly dark at the center, especially at its apex and was surrounded by bright boundaries. On a larger scale, the smectic liquid crystal layer appeared to be divided into a few larger regions, in each of which could

be formed the fan-shaped texture with a definite orientation of the long axes. The darkness and the brightness of the larger regions changed alternately as one of the polaroids was rotated. More careful investigations revealed that there was a dark spiral protruding from the apex of each long axially-symmetric region. The fan-shaped textures, with the small domains and their spirals are shown in Fig.25 and Fig.26 for PCBAV at temperatures 72.3 ^{o}C and 106.2 ^{o}C respectively, both with sample thickness of 100 μm.

Another modification of the focal-conic texture could also be obtained under conditions very similar to that which produced the fan-shaped texture already described. This texture was in many respects similar to the fan-shaped texture although the focal conics were much shorter. Each focal conic was divided by two crossed dark lines into four smaller regions. In crossed polaroids, only the regions in the vicinity of the dark lines were quite dark whereas the others were fairly bright and the darkness changed uniformly from the dark lines to the boundary. Both the fan-shaped texture and the latter kind of focal-conic texture looked rather flat, with smooth, slightly curved surfaces. The boundaries in these textures never intersected one another but only met tangentially and their long axes tended to point preferentially in the same direction.

When the temperature of the smectic liquid-crystal layer was raised to a few degrees below the smectic-isotropic transition point, the focal-conic textures started to change slowly to the polygonal texture. The growth rate depended mainly on the temperature, the closer to the transition temperature, the larger the growth rate. The polygons were in many respects similar to the spherulites obtained in

polymer crystallization. They grew larger and larger until they touched each other and then stopped growing. They never invaded one another and left the areas between them as homogeneous regions as shown in Fig.27 for EEBAC at temperature 140.^{o}C with a sample thickness of 100 μm. As shown in Fig.28 the polygons grew larger a few minutes later.

It should be noted that the polygonal textures also occurred frequently in the supercooled state of smectic liquid crystals. As the isotropic phase was cooled down to below the smectic-isotropic transition temperature and thus the smectic liquid crystal was in the super-cooled state, some small focal-conic textures were first obtained. These focal conics could then coalesce to form some long, irregular regions, known as bâtonnets. Their shapes and sizes could vary widely. When the temperature was lowered far below the transition temperature, the bâtonnets became larger and larger and also more clouded.

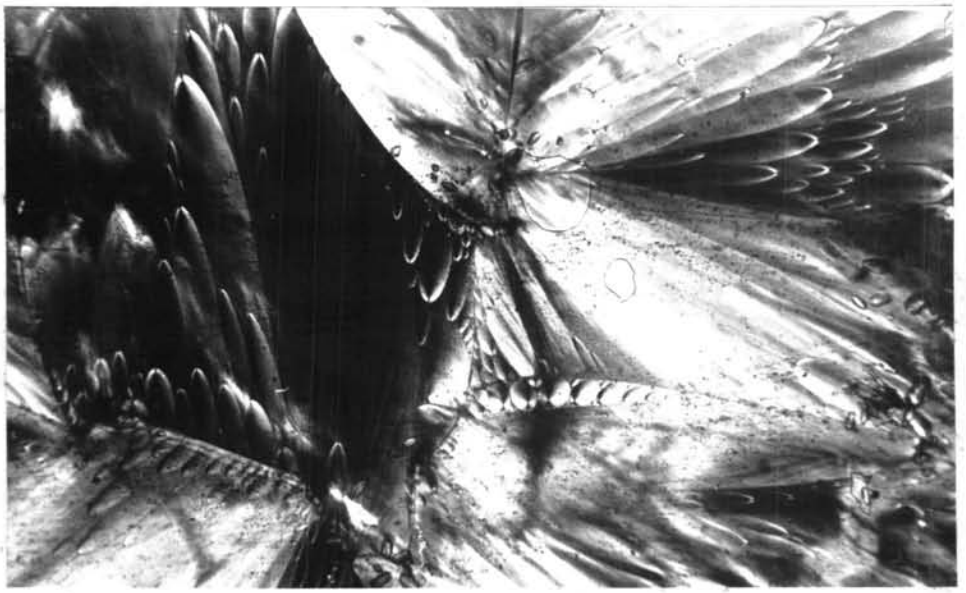

Fig.25 Fan-shaped texture of PCBAV at temperature 72.3 °C

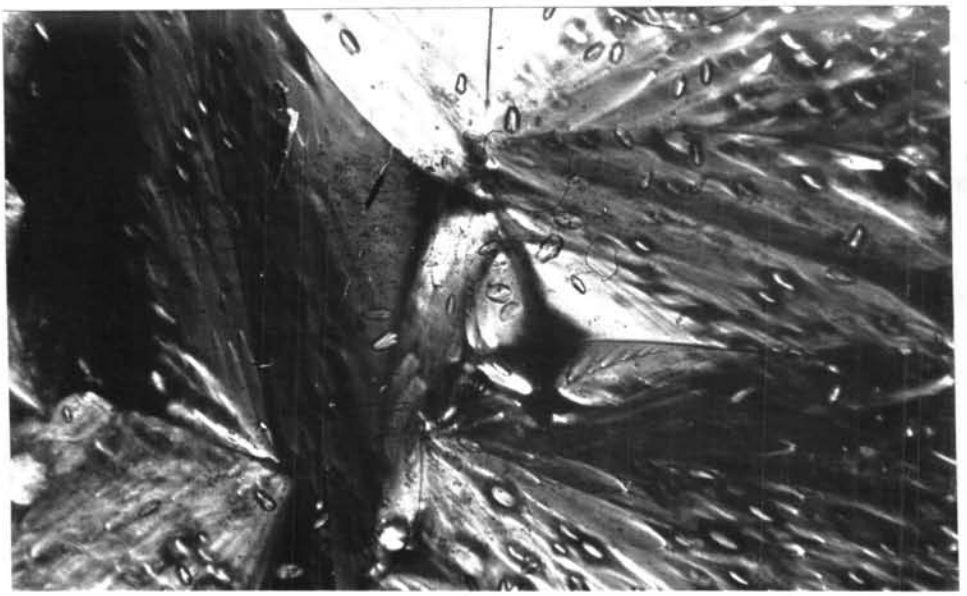

Fig.26 Fan-shaped texture of PCBAV at temperature 106.2 °C

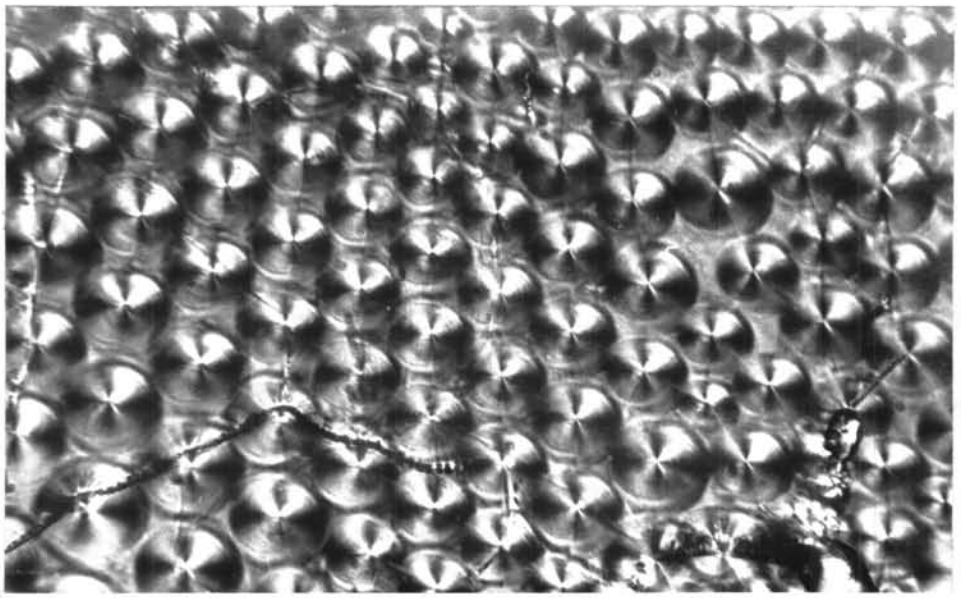

Fig.27 Polygonal texture of EEBAC at temperature 140 °C

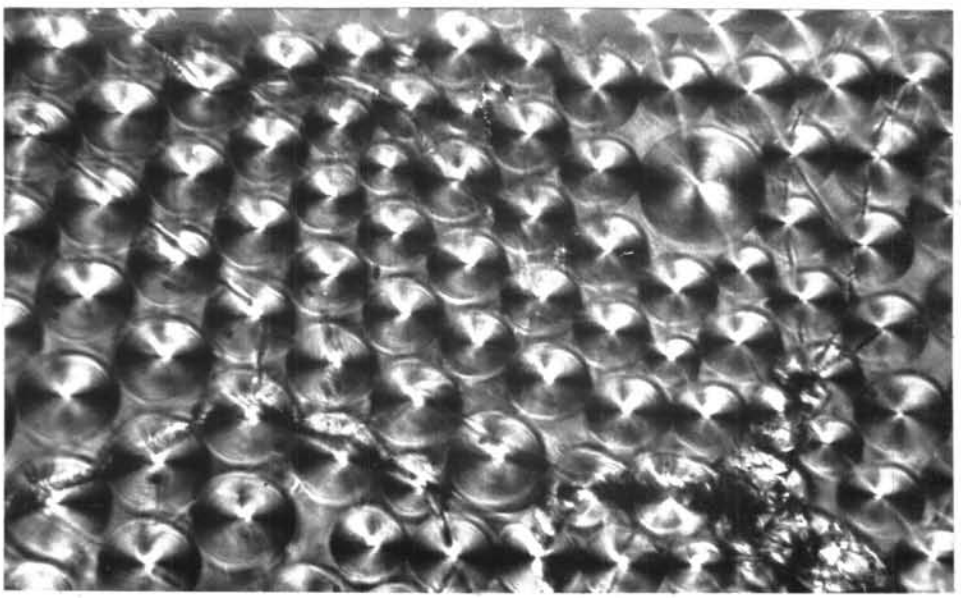

Fig.28 Polygonal texture of EEBAC at temperature 140 °C

II.6.6 Motions of smectic liquid crystals placed between transparent electrodes

In the presence of an electric field the motions in smectic liquid crystals were found to be entirely different from those previously described for the case of nematic liquid crystals. Instead of the domain motions, a high field strength of about 10^4 volts/cm was required for textural motions. The focal conics which are usually found in a smectic liquid crystal became slightly elongated and slid perpendicular to the field direction towards some regions especially the boundary of the drop, as illustrated in Fig.29 for PCBAV in an a.c. field of 2.2×10^4 volts/cm, temperature 94.0 °C, with a sample thickness of 100 μm. The velocity of sliding was found to be roughly proportional to the field strength. As the field was raised further, this motion was coupled with a rotation around the long axes of the focal conics. The angular velocity was approximately proportional to the field strength. If the temperature was increased towards the smectic-isotropic transition point, the focal conics split into a number of much smaller focal conics. The splitting became more vigorous at higher field strengths. More careful observations indicated that the splitting resulted from a vigorous rotation about the long axes.

When the smectic liquid crystal was cooled down from the isotropic phase to the isotropic-smectic transition point, in this supercooled state, both d.c. and a.c. field induced the formation of focal conics as shown in Fig.30 for EEBAC in an a.c. field of 1.0×10^4 volts/cm, temperature 150.4 °C, sample thickness 100 μm and in Fig.31 for PCBAV in a d.c. field of 2.5×10^3 volts/cm, temperature 100.3 °C, with a sample thickness of 100 μm. These focal conics

frequently adhered together to produce bâtonnets, larger focal conics or to adhere to previously formed polygons, as shown in Fig.31 . Frequently, rod-shaped texture was formed in the supercooled state as illustrated in Fig.32 for PCBAV at a.c. field of 5.0×10^3 volts/cm, temperature 104.1 ^{o}C, with a sample thickness of 100 μm. The effects of an electric field on the bâtonnets, the rod-shaped texture and the focal conics were to cause a rotation around their long axes and a vibration about the field direction. At higher field strengths, the focal conics or the polygons burst violently into a number of much smaller focal conics because of the vigorous rotation of each small focal conic as shown in Fig.33 and Fig.34 at a.c. field of 7.2×10^3 volts/cm, temperature 103.6 ^{o}C, and at a.c. field of 1.5×10^4 volts/cm, temperature 96.4 ^{o}C, both with sample thickness of 100 μm of PCBAV.

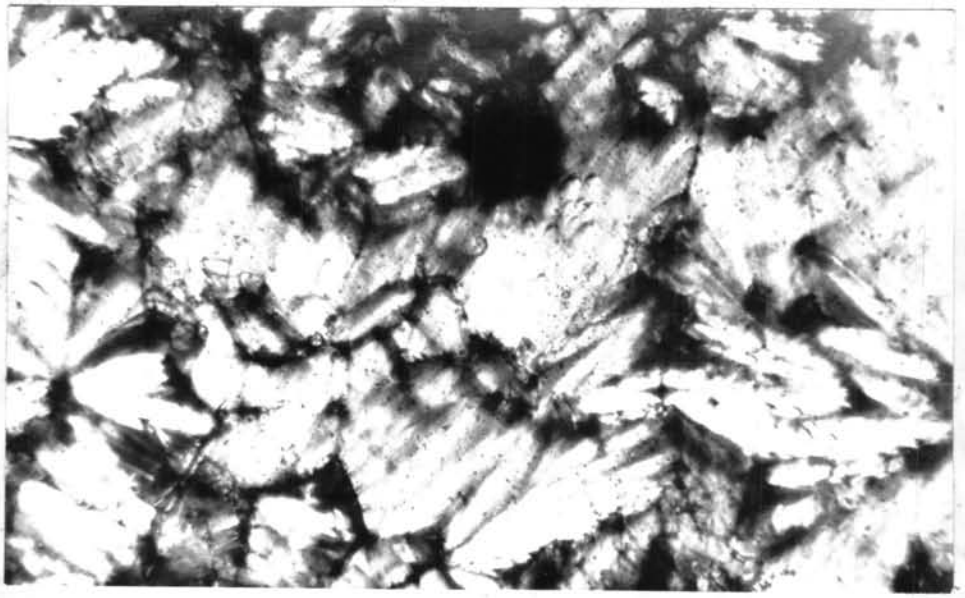

Fig.29 A 100 μm-thick layer of PCBAV placed between transparent electrodes in an a.c. electric field of 2.2×10^4 volts/cm at 94.0 °C.

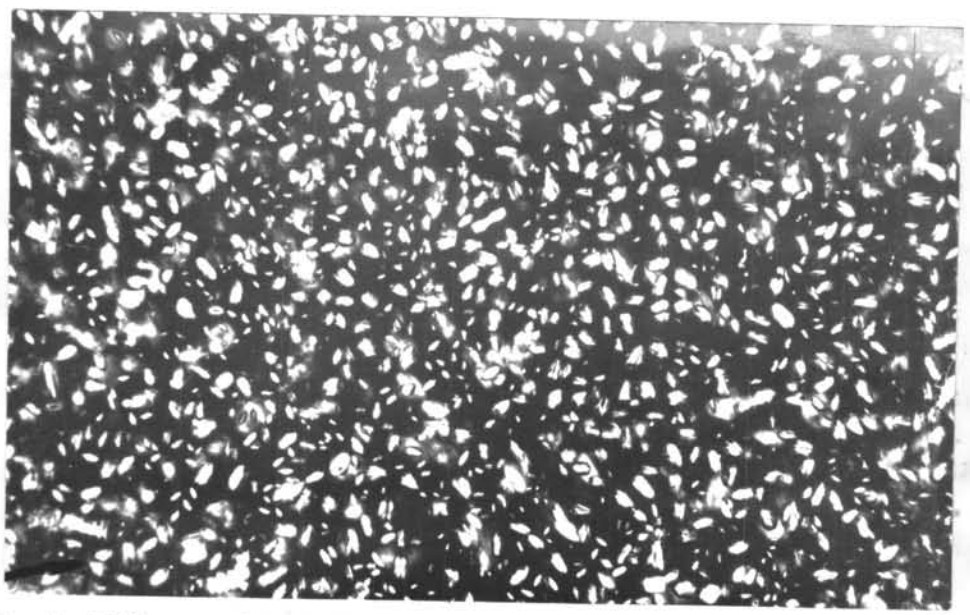

Fig.30 A 100 μm-thick layer of EEBAC placed between transparent electrodes in an a.c. electric field of 1.0×10^4 volts/cm at 150.4 °C.

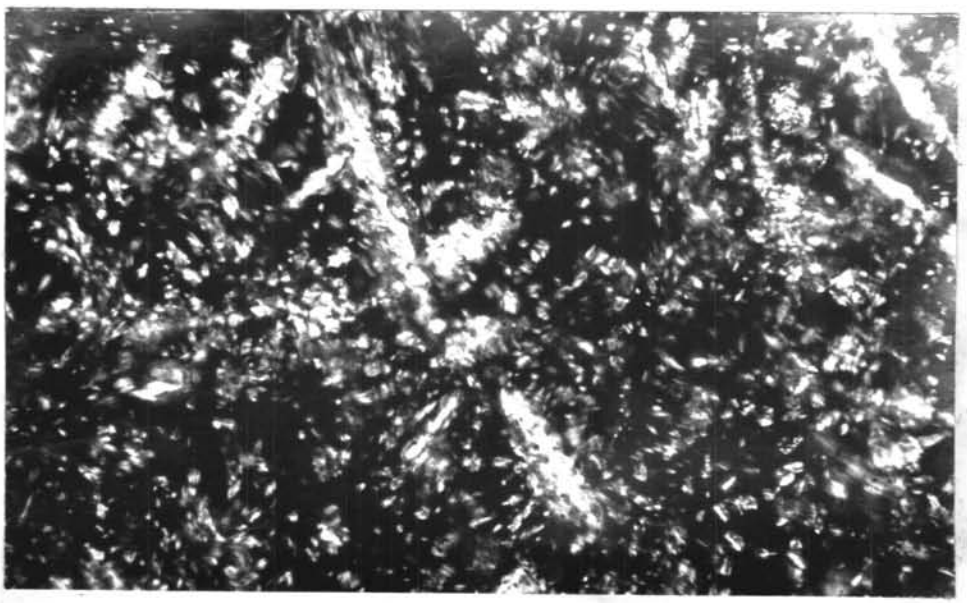

Fig.31 A 100 μm-thick layer of PCBAV placed between transparent electrodes in a d.c. electric field of 2.5×10^3 volts/cm at 100.3 ^{o}C.

Fig.32 A 100 μm-thick layer of PCBAV placed between transparent electrodes in an a.c. electric field of 5.0×10^3 volts/cm at 104.1 ^{o}C.

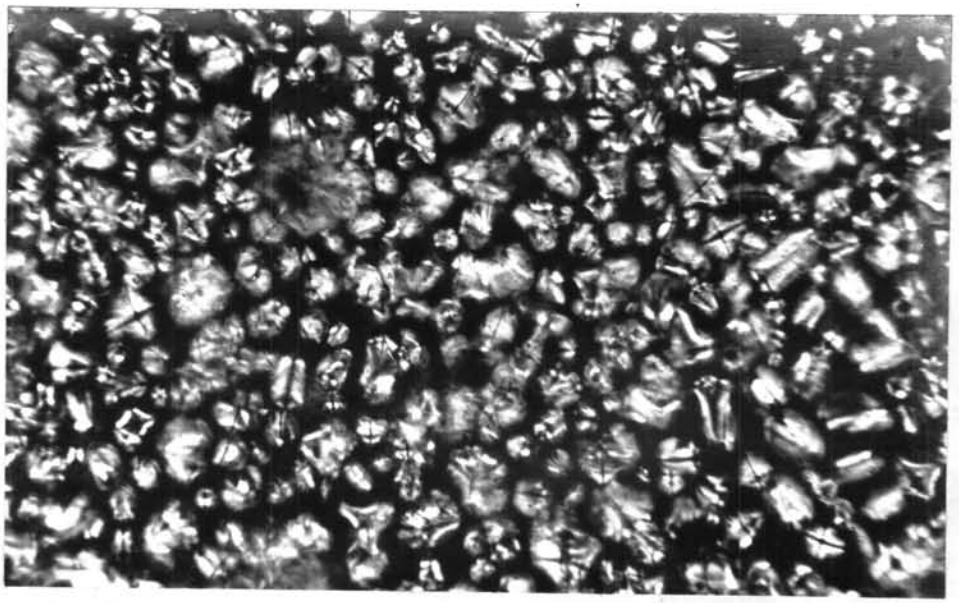

Fig.33 A 100 μm-thick layer of PCBAV placed between transparent electrodes in an a.c. electric field of 7.2×10^3 volts/cm at 103.6 ^{o}C.

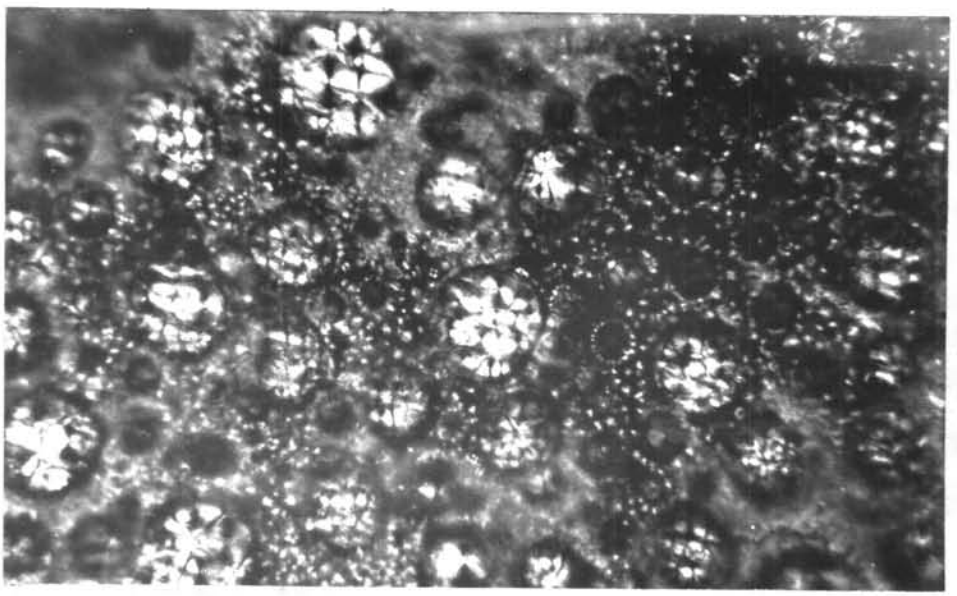

Fig.34 A 100 μm-thick layer of PCBAV placed between transparent electrodes in an a.c. electric field of 7.2×10^3 volts/cm at 96.4 ^{o}C